



## NATURAL BACKGROUND RADIATION IN JORDAN

M.N.S. DAOUD

National Resources Authority,  
Ministry of Energy and Mineral Resources,  
Amman, Jordan

### Abstract

An Airborne Gamma Ray survey has been accomplished for Jordan since 1979. A complete report has been submitted to the Natural Resources Authority along with field and processed data "digital and analogue". Natural radioelements concentration is not provided with this report. From the corrected count rate data for each natural radioelement, Concentrations and exposure rates at the ground level were calculated. Contoured maps, showing the exposure rates and the dose rates were created. Both maps reflect the surface geology of Jordan, where the Phosphate areas are very well delineated by high-level contours. In southeastern Jordan the Ordovician sandstone, which contain high percentage of Th (around 2000 ppm in some places) and a moderate percentage of U (about 300 ppm), also show high gamma radiation exposures compared with the surrounding areas. Comparing the values of the exposure rates given in ( $\mu\text{R/h}$ ) to those obtained from other countries such as United States, Canada, Germany, etc. Jordan shows higher background radiation which reach two folds and even more than those in these countries. More detailed studies should be performed in order to evaluate the radiological risk limits on people who are living in areas of high radiation such that the area of the phosphatic belt which covers a vast area of Jordan high Plateau.

### 1. INTRODUCTION

The natural environment is the major source of radiation exposure to man. This natural radiation could be used as a standard for comparing additional sources of man made radiation such as those produced by medical sources of X rays, atomic weapons, fallout, nuclear power generators and radioactive waste disposal. To assess the significance of these additional sources of man-made radiation, the levels of natural background radiation and its variation must be known. Radiation exposure is considered as internal when it is taken by breathing or swallowing such as  $^{40}\text{K}$  or  $^{222}\text{Rn}$  and it is considered as external when it is received by the surface of the body such as cosmic rays and natural radioactive elements principally  $^{40}\text{K}$  and uranium and thorium decay series occurring in the ground, in building materials and in the air.

The external radiation can vary considerably according to many things such as the geological environment, the elevation above the sea level, the temperature, humidity, moisture, type of living and accommodation, etc.

The natural radionuclides decay through emission of alpha particles, beta particles and gamma radiation. Alpha particles are very heavy and cannot travel more than few centimeters through the air. Beta particles which are much lighter can travel about one metre in the air. While gamma rays which have almost no mass can travel several hundred metres through the air. Cosmic rays which are very energetic can travel long distances from stars and penetrate the whole earth's atmosphere down to the ground surface. While lungs and respiratory tract are the most affected organs to alpha and beta particles which are present in the air, except that the human body is exclusively exposed to gamma and cosmic radiation.

This report deals with the effects of gamma radiation, emitted only by the natural radioelements of potassium and uranium and thorium and their decaying series, on the whole body and is not concerned with alpha and beta particles which affect only specific parts of the body. Different kinds of techniques were used to evaluate the natural background radiation in different parts of the world; these techniques have involved the use of ionization chambers, portable and airborne scintillometers, laboratory analysis of the radioactive elements in soil samples, etc. None of these above methods was capable to carry out a representative sampling on a country wide basis because

of the variation of the ground radioactivity from place to place and because of the limited number of measurements that could be taken.

Because of the large areas that could be covered and the huge amounts of data that could be collected, airborne survey is considered as unchallenged method in the point of view representation. Very considerable improvements were achieved since the first airborne radiometric surveys until recent airborne gamma ray spectrometer surveys. Improvements did not involve only the equipment, where powerful computers control the whole parameters of the flight with very sophisticated equipment on board, but the procedure as well which includes the construction of large radioactive concrete calibration pads and the establishment of airborne calibration range such that of Breckenridge strip near Ottawa in Canada. Now it is possible to estimate the concentration of the natural radioelements at the ground level with high accuracy.

## 2. GEOCHEMISTRY OF RADIOELEMENTS

It is important to know the distribution of the natural radioelements in nature in order to know which rock type is responsible of the most contribution of gamma radiation to the environment. This will lead us to have a certain knowledge about the abundance of these radioelements in nature.

### 2.1. Abundance in crustal rocks

Table I indicates the concentration of the three radioelement in common rock types. All three elements are oxyphile and have relatively large ionic radii, these two factors play a role in the crystal chemistry. Within igneous rocks, the abundance of the three radioelements increases with increasing silica content. The difference in geochemical behaviour becomes apparent under strongly oxidizing conditions which may exist beyond the stage of pegmatite formation, or under supergene conditions. Uranium and Thorium behave in a similar way when uranium exists in a quadrivalent state which is the characteristic of uranium, and form several isomorphous mineral series, but uranium behaves differently in the hexavalent state. Both elements may occur as accessory minerals in granitoid rocks or be concentrated in pegmatite.

TABLE I. RADIOELEMENTS CONCENTRATIONS IN CRUSTAL ROCKS  
[Adapted from Clark et al. (1966)]

Rock type	K %	U (ppm)		TH (ppm)		Th/U	
	average	average	range	average	range	average	range
crustal average	2.1	3		12		4	
mafic igneous	0.5	1	0.2-3	3	0.5-10	3	3-5
intermediate igneous	1-2.5	2.3	0.5-7	9	2-20	4	2-6
acid igneous	4	4.5	2-23	28	5-20	4	2-10
arenaceous sediment	1.4	1	0.5-2	3	2-6	3	
argillaceous sediment	2.7	4	1-13	16	2-47	4	1-12
limestone	0.3	2	1-10	2	-	1	
black shales	2.7	8	3-250	16	-	2	wide
laterites	low	10	3-40	50	8-132	5	wide
metamorphics		depend on rock type					

## **2.2. Uranium Geochemistry**

The relative concentration of uranium compared to both thorium and potassium is an important factor in the recognition of possible uranium deposits using gamma ray survey. In the hexavalent state, uranium is ready to form the soluble uranyl ion ( $\text{UO}_2^{++}$ ) and become very mobile. This permits the segregation and, under favourable conditions, the concentration of the uranium. More commonly, uranium moves in solution as the uranyl complex with carbonate, sulphate and chloride ions. Under reducing conditions, the uranyl is precipitated as primary complex oxide compounds by organic matter or insoluble hydroxides of iron or manganese. Under oxidizing conditions, secondary uranium minerals are precipitated by evaporation of uranium bearing solutions, and with copper, calcium, potassium or other metals may form as phosphates, arsenates, vanadates or silicates. Black shales and marine phosphates are commonly enriched in uranium and may contain in excess of 100 ppm. Gamma ray measurements of uranium abundance usually depend upon the gamma emission of its daughter product,  $^{214}\text{Bi}$ , which is the ninth decay product in the series. Radon and radium are very important in geochemistry exploration because of their mobility. Radium is only mobile in sulphate free, neutral or acid solutions and is ready to be precipitated by gypsum, anhydrite, barite, hydroxides of iron, manganese and aluminium. Radon on the other hand is an inert gas with a short half-life time but is easily dissolved in water and can escape to the atmosphere through permeable rocks. The displacement of uranium, radon or radium from the mother radioactive source will cause disequilibrium, leading to erroneous gamma ray estimations of the uranium concentration in the source, and may create confusing secondary exploration targets in the vicinity.

## **2.3. Thorium Geochemistry**

There is similarity of geochemical behaviour for both uranium and thorium under hypogene conditions. Thorium is not susceptible to leaching under most supergene conditions, and its principal mode of occurrence is in the refractory heavy minerals, which under supergene conditions may become concentrated as residual residue in laterite cappings, or in placers deposits. In primary igneous rocks some carbonatites are strongly enriched in thorium, which is indicative of the presence of other rare earth's.

## **2.4. Potassium Geochemistry**

The geochemistry of potassium is well known and may need to add this comment. Certain types of uranium mineralization are accompanied by sodium metasomatism mineralization. Under these conditions sodium initially replaces potassium in rock forming minerals and further exaggerates the U/K ratio which always increases where there is significant uranium mineralization.

# **3. AIRBORNE RADIATION SURVEY OF JORDAN**

## **3.1. Survey planning**

The survey, which covered the entire Kingdom of Jordan, was divided into three zones as illustrated in Fig. 1. All lines were flown in an east northeast/west southwest direction as indicated on the flight path map Fig. 2. Survey lines were planned to terminate 8 kilometers from the international borders. Area A is only a magnetic survey area which covers the Wadi al Araba-Jordan Rift and the highlands east of the rift, including the outcropping basement rocks of the southern mountainous desert. The flight altitude was kept constant for each traverse within area A varying between 1500 and 2000 metres above sea level, depending on the maximum height of the topography beneath the flight line. ENE traverses were spaced at 1 km intervals with NNW control lines flown at 20 km spacing. Control lines were also flown along the western and southern perimeters of the

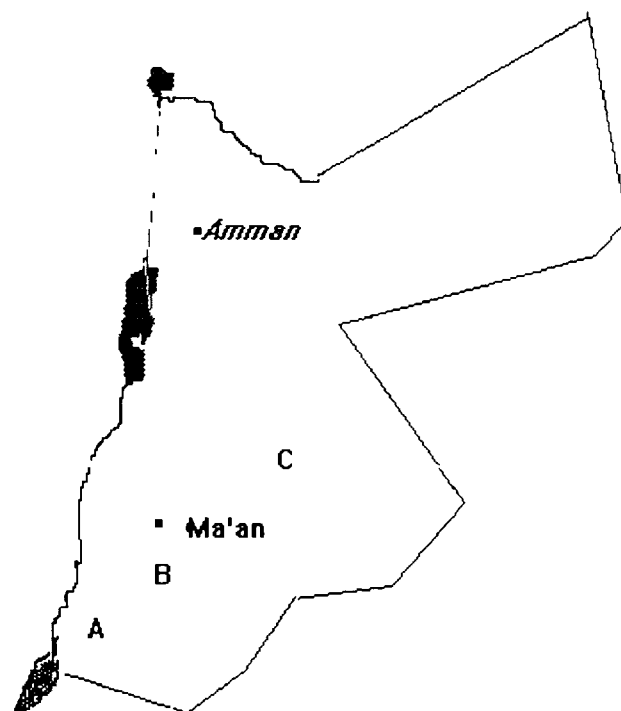


FIG. 1. Location map of the survey area

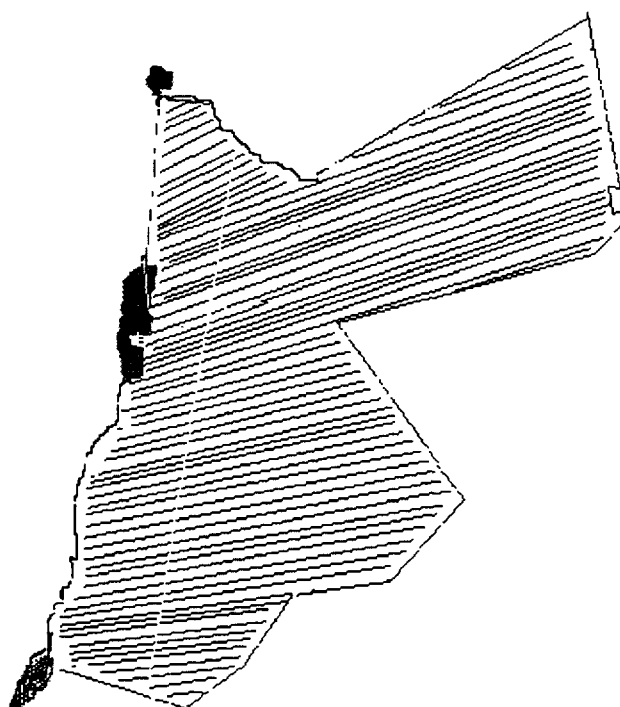


FIG. 2. Flight path map

area. Area B, as depicted in Fig. 1 is a magnetic and gamma radiation survey area. A survey altitude of 120 metres terrain clearance was maintained except over a small section in the north-west corner where rugged topographic features necessitated flight altitudes of 800 to 1050 metres above sea level in order to ensure safe aircraft operations. ENE traverses were spaced at 1 km intervals with NNW control lines at 10 km interval in the northern section of the area and 20 km intervals in the southern

portion. Three NS traverses were flown along the western boundary of the survey area, from the southern end of the Dead Sea to the northern survey limit in order to ensure complete survey coverage.

Area C, a magnetic and gamma radiation survey area, covered the largest portion of the Kingdom of Jordan as shown in Fig. 1. A survey altitude of 120 meters terrain clearance was maintained for the entire area. ENE traverses were spaced at 2 km intervals with NNW control lines flown at 20 km spacing and 2 perimeter control lines were flown across the northern boundary. The bases of the survey operation were Amman for the northern portion of the survey and Aqaba for the southern portion. The survey aircraft was a twin-engine Douglas DC-3 with registration C-FITH.

The equipment on board the aircraft used for the purpose of the survey are described as list-1.

*List 1: Airborne Survey Equipment*

- Airborne Magnetometer-Geometric Model G803 proton precession magnetometer with sensor mounted in a tail stinger. The magnetometer resolution was 0.5 gauss with a sampling interval of 1.0 second.
- Crystal Detectors- 8 Harshaw polycrystalline  $10.2 \times 10.2 \times 40.6$  cm Sodium Iodide (Thallium activated) crystal. Total crystal volume of 33567 cubic centimeters.  
Geotrex MADACS digital data acquisition computer system. Basic components are an Interdata Model 6/16 minicomputer, a crystal clock, a Nuclear Data Model 560 analogue/digital converter and custom designed operating system.
- Digi Data Model 1600, 9 track, 800 BPI magnetic tape transport.
- Gulton Model TR-888, 8 channel analogue chart recorder (4 cm/channel).
- Moseley Model 7100B, 2 channel analogue chart recorder (25.4 cm width).
- Geotrex Model 75-SF, 35 mm frame, tracking camera.
- Sperry Radar Altimeter, Model RT-220.
- Geotrex custom magnetometer compensation unit.
- Bendix DRA-12C Doppler navigation system.

### **3.2. Data Acquisition**

Doppler navigation was employed in addition to visual navigation through the use of topographic map flight strips. Visual navigation alone has been impractical as a large portion of the survey area was desert area devoid of identifiable features.

The recording of all of the airborne survey parameters was controlled by a command signal from the MADACS unit. MADACS is the name of a Geotrex designed software controlled system built around a 16-bit minicomputer. This unit controlled and synchronized the recording of all the parameters through a crystal clock. The spectrometer system recorded the radiometric counts in 256 channels for energies in the range 0.0 to 3.0 Mev.

Also recorded were four channels of summed "window" data for the energy ranges as indicated in Table II.

TABLE II. 4 GAMMA- RAY WINDOWS RECORDED BY GEOTERREX SPECTROMETER SYSTEM

Window	Photo Peak	Energy Range (Mev)
Thorium	Thallium 208	2.42–2.82
Uranium	Bismuth 214	1.66–1.86
Potassium	Potassium 40	1.36–1.56
Total Count	—	0.8–2.82

The spectrometer magnetometer, radar altimeter and barometric altimeter data were recorded in both analogue and digital formats with no corrections applied. On the 8 channel analogue recorder, each channel is 4 cm and the chart speed was 6.0 cm/minute. A sample of an 8 channel analogue record is contained in Fig. 3. The parameters recorded and their full scale deflections, arranged in order of chart top to chart bottom, are described as list 2

*List 2. Survey parameters and their full scale deflections*

Integer Fiducials	every 10 samples (10 seconds)
Barometric Altimeter	1000 feet deflection (305 metres)
Radar Altimeter	1000 feet deflection
Magnetics(coarse scale)	2000 gamma deflection
Magnetics (fine scale )	200 gamma deflection
Total Counts	2000 counts/second deflection
Potassium	500 counts/second deflection
Uranium	200 counts/second deflection
Thorium	200 counts/second deflection

The Doppler measurements, recorded in digital format only, were the instrument output before processing through the Doppler navigational computer. Hence they were not subject to any changes made by the pilot in his instrument settings. The two parameters recorded digitally were the distance traveled and the track direction, in each one second measuring interval.

### 3.3 Survey Procedures

#### 3.3.1. Geophysical Equipment Tests

The following tests of the geophysical survey instruments were made: Prior to departure for Jordan the radiometric instruments had been calibrated on the radiometric test pads and over the range near Ottawa, Canada. The results are included with Phoenix report. After arrival in Jordan, on the ground and before each survey flight, a radiometric balance check and adjustment was performed under control of the MADACS operating system.

#### 3.3.2. Flight Tests

Prior to the commencement of flying the actual survey portion of a flight and just after, a series of short tests were performed for the purpose of monitoring the equipment stability and for calibration. A common test line, which was selected for repeatability of navigation and geophysical responses was flown with all survey equipment in operation. While based in Amman, the test line was over a railroad line just south of Amman ending just before the new airport under construction. While

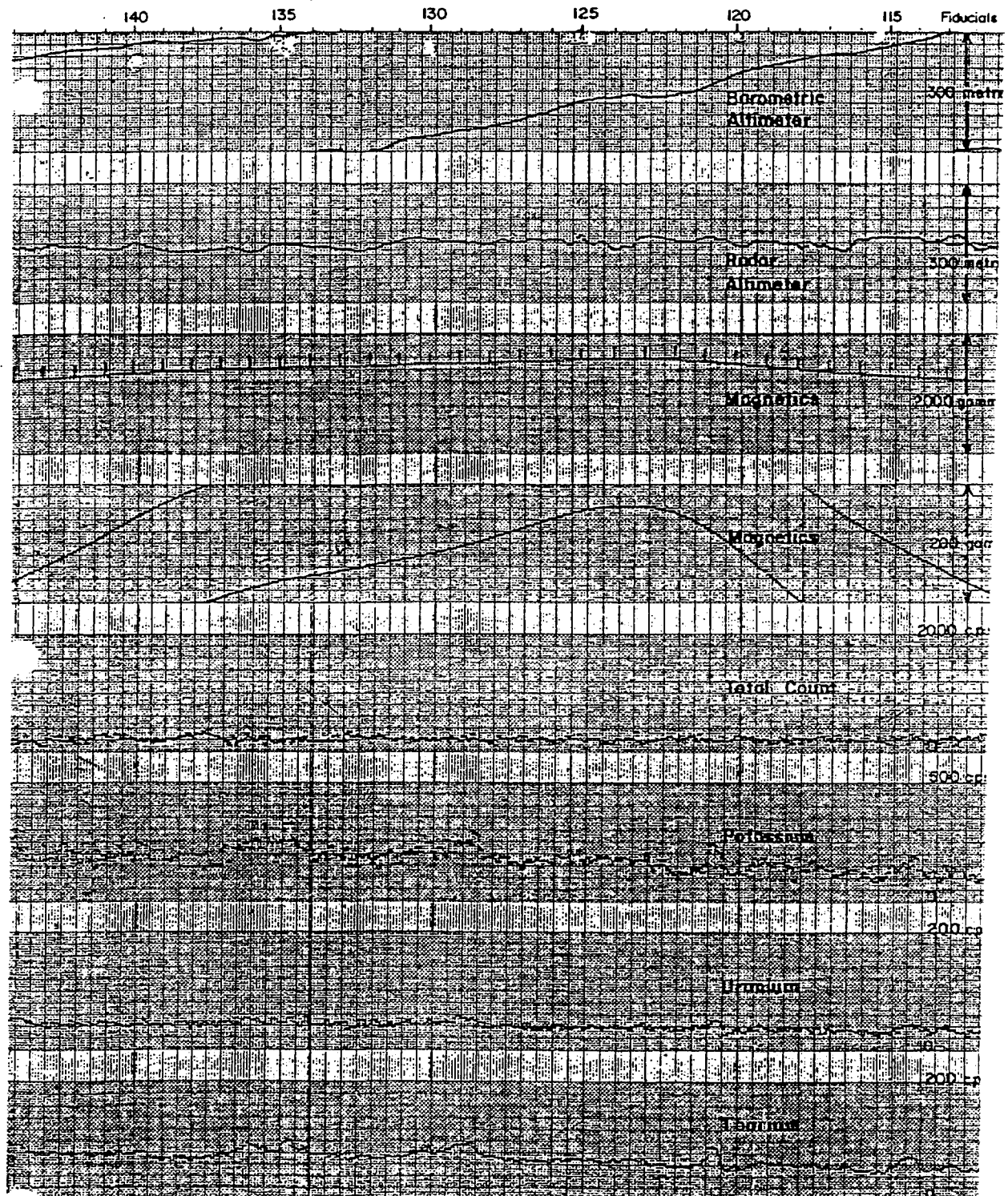


FIG. 3. Sample of eight channel analogue record (not fit to scale).

based at Aqaba airport the test line was flown over the gulf of Aqaba. Backgrounds are best determined by flying over a large body of water at survey altitude but in the north this was impossible. General checks for the proper functioning of all inputs to the MADACS system (barometric altimeter, radar altimeter, tracking camera, Doppler, radiometric sensors) were made before commencement of surveying.

The MADACS system, under control of the operator, was capable of providing on-line multichannel display of accumulated natural Potassium and Thorium photopeaks.

### *3.3.3. Post flight Procedures*

Upon completion of a flight, the 35 mm tracking was developed. The actual flight path was proved by identifying points from the film on the topographic map flight strips. Flight log and analogue records were checked to ensure the satisfactory data had been obtained. The radiometric source tests and test line results were analyzed to check the stability of the spectrometer system. All original survey data, analogue or digital, have been delivered to Natural Resources Authority.

## **3.4. Aeroradiometric Data Reduction and Compilation**

In order to relate the airborne count rates of the three windows to radioelement concentrations of the ground four distinct steps are necessary: the removal of background radiation; the spectral stripping procedure; altitude correction; with temperature and pressure correction; and the conversion of the corrected count rate data to ground concentration.

### *3.4.1. Removal of Background Radiation*

Three sources of background radiation exist in any airborne radioactivity measurements:

the radioactivity of the aircraft and its equipment; cosmic radiation; and the radioactivity in the air arising from daughter products of radon gas in the uranium decay series. To remove the effect of these three sources, it will be enough to take measurements over a large body of water. Unfortunately large bodies of water are not available except the Dead Sea and Aqaba Gulf.

When the survey was based in Aqaba, the background calibrations were made at survey altitude over the gulf of Aqaba. While the survey based in Amman, the aircraft flew at high altitude. The backgrounds, which were subtracted from the survey data, were determined linearly interpolating on a time basis from the pre-flight to the post-flight background levels.

### *3.4.2. Stripping Procedure (Compton Stripping Factors)*

Due to the characteristics of the airborne gamma ray spectrum measured by sodium iodide detectors, gamma rays emitted from one particular radioelement may be detected in the other two windows. To correct for this interference, a spectral stripping procedure must be carried out. This is achieved by calibrating the aircraft and equipment over a set of large radioactive concrete pads which were constructed at Uplands Airport in Ottawa, Canada. The calibration pad measurements were carried out on August 31, 1979. Mean total system count rates observed in the Total Count, Potassium, Uranium and Thorium are summarized in Table III. These mean values were used for the calculation of the stripping constants.

The Compton stripping coefficients are ( $\alpha$ ,  $\beta$ ,  $\gamma$ , a, b and g) and error analyses of these values were computed using the mean window count rates previously described. Calculations of the above coefficients were performed after the Tammenmaa program utilizing a weighted fit to all six stripping ratios, the matrix used in the calculation is having the following form.

K3	a	b	B1
$\alpha$	K2	g	B2
$\beta$	$\gamma$	K1	B3

Where K represents the test pad sensitivities;  
 $\beta$  represents the window background estimates;  
1, 2, 3 represent Potassium, Uranium and Thorium windows respectively.

The compton stripping coefficients extracted from running this programme are:

$\alpha$  (Th into U) = 0.36648  
 $\beta$  (Th into K) = 0.44650  
 $\gamma$  (U into K) = 0.76596  
a (U into Th) = 0.01742  
b (K into Th) = 0.01110  
g (K into U) = 0.01398

TABLE III. LIVE TIME NORMALIZED COUNT RATES

Test pad number	Total Count (cps)	Potassium (cps)	Uranium (cps)	Thorium (cps)	Recording Time (sec)
1	1782.8	443.8	95.8	85.9	610
2	2784.3	619.6	118.9	119.7	641
3	2974.7	598.9	165.3	221.1	611
4	3753.9	657.9	208.6	339.6	631
5	3242.0	667.3	248.5	122.3	609

### 3.4.3 Altitude Correction

One of the factors that affects the number of gamma rays detected per second in each window (N) is the altitude of the aircraft above the ground. It is found experimentally that the stripped and background-corrected count rate in each window is to be related to the aircraft altitude (H) by a simple exponential expression of the form:

$$N = A e^{(-\mu H)} \quad (1)$$

where A and  $\mu$  are constants.

Fig. 4 shows the stripped and background-corrected potassium count rate variation with aircraft altitude over the GSC airborne gamma ray spectrometer calibration range at Breckenridge 30 km west of Ottawa, flown by Douglas DC-3 on August 31, 1979. The exponential curve given by the above equation is also shown. This curve is used to correct the count rates in each window for deviations from the planned survey altitude. The detailed description of the algorithm used in the reduction of the Jordanian radiometric data is shown in Annex No. 1. It takes into consideration the previous corrections.

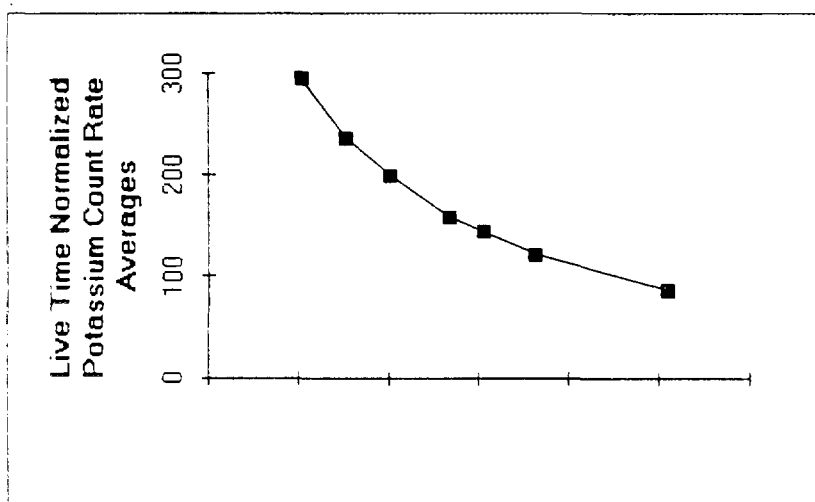


FIG. 4. Potassium count rate variation with aircraft altitude.

From the measured ground radioelement concentration of the calibration range the sensitivity of the airborne gamma ray spectrometer in terms of counts per unit time per unit concentration of potassium, uranium and thorium may be determined at the nominal survey altitude, thus allowing the ground concentration to be evaluated over unknown area. As the twin-engined Douglas DC-3 aircraft flew over the GSC airborne calibration range at different altitudes on August 31, 1979 which has a known concentration, it was possible to establish a relationship between the stripped background-corrected count rates and the concentrations of the natural radioelements at the ground level.

In an attempt to establish a relationship between the field measurements and laboratory analyses; 70 soil samples were collected at seven sites along the 10 km length of the strip [Grasty, 1975]. These samples were then sealed in metal cans, stored 4 weeks to allow the gamma ray activity of  $^{214}\text{Bi}$  to reach equilibrium, and analysed in the laboratory by gamma ray spectroscopy for potassium, uranium and thorium. These results are presented in Table IV, together with the results of a detailed ground gamma ray spectrometer survey carried out with a portable spectrometer calibrated on the radioactive concrete calibration pads at Uplands Airport in Ottawa [Charbonneau and Darnley, 1970] concrete calibration pads at Uplands Airport in Ottawa [Charbonneau and Darnley, 1970].

TABLE IV. RADIO-ELEMENT CONCENTRATION OF THE BRECKENRIDGE AIRBORNE CALIBRATION RANGE

Type of measurement	Number of analyses	Potassium (%)	Uranium <sup>1</sup> (ppm)	Thorium <sup>1</sup> (ppm)
Laboratory (sealed can assay)	70	$2.03 \pm 0.04$	$0.92 \pm 0.09$	$7.70 \pm 0.28$
Field	27	$1.8 \pm 0.1$	$0.5 \pm 0.1$	$8.0 \pm 0.4$
Assigned value		$2.03 \pm 0.04$	$0.5 \pm 0.04$	$7.70 \pm 0.28$

<sup>1</sup> Assuming radioactive equilibrium

Field and laboratory measurements show good agreement for potassium and thorium. Contrary to the uranium laboratory assays which are considerably higher than the field measurements. These results could be explained by a loss of  $^{222}\text{Rn}$  from the surface soil of the calibration strip and a corresponding decrease in the  $^{214}\text{Bi}$  activity. In the case of laboratory assays the radon and associated  $^{214}\text{Bi}$  activity is allowed to build up and reach equilibrium because the cans are sealed and the radon gas cannot escape. Exposure rate above the ground, due to gamma rays emitted by the uranium series, is better estimated by field gamma ray spectrometer measurements rather than laboratory assays on sealed samples which can indicate an artificially high gamma ray activity. The equivalent uranium concentration of the test strip was therefore assigned the field value of  $0.5 \pm 0.1$  ppm. Thorium and potassium laboratory were considered more reliable than the field measurements because of the greater number of samples analysed (see Table IV). Based on the potassium, uranium and thorium count rates recorded over the strip and the calibration pads, the sensitivities of the 8 Harshaw polycrystalline Sodium Iodide (Thallium activated) crystal were evaluated by Phoenix and values are given in Table V including other two detectors from GSC for comparison of the sensitivities of the two GSC detectors with the Harshaw detector supplied by Phoenix.

TABLE V. SENSITIVITY FOR DIFFERENT TYPES OF SODIUM IODIDE CRYSTALS

System	Potassium per K%	Uranium (ppm)	Thorium (ppm)
12 ( $22.9 \times 10.2$ cm) Cylindrical detector	$78.9 \pm 4.2$	$19.1 \pm 4.8$	$6.1 \pm 0.4$
12 ( $12.2 \times 10.2 \times 40.6$ ) Prismatic detector	$90.9 \pm 1.8$	$16.2 \pm 0.9$	$7.0 \pm 0.1$
8 ( $10.2 \times 10.2 \times 40.6$ ) Prismatic detector Harshaw	$66.5 \pm ?$	$7.7 \pm ?$	$4.8 \pm ?$

#### 4. RADIATION DOSES UNITS

All people are exposed to gamma radiation resulting from radioactivity, and it should be recognized that the biological long-term effects of such an exposure are unknown and may be detrimental. Units of radioactivity can be confusing. This confusion originating from the fact that an ionizing field of radiation cannot be defined uniquely, such as the case of almost all fields of science, since it can consist of radiation with a complete range of energies and angular distributions. One way of comparing radiation fields is by means of an ionization chamber which measures the quantity of electrical charge released in a gas through absorption of the radiation. This type of measurement is most useful for the health physicist since it may be related to the physical damage that will occur in living cells. The radiation intensity at a given place is termed its "Exposure" (E) and is measured by its ability to produce ionization at that place; the unit of exposure is the roentgen. One roentgen is defined as the quantity of X or gamma radiation that produces one electrostatic unit of charge of either sign in 1 ml of air at standard temperature and pressure. The unit of "absorbed energy" or "dose" is the energy imparted by ionizing radiation to 1 gram of any material at the particular point of interest. The unit of absorbed dose is the "rad" (Radiation Absorbed Dose) which is deposition of an energy of 100 ergs per gram. In expressing the absorbed dose, the particular absorbing material under consideration must always be given. Environmental radiation measurements are normally presented as absorbed dose rates in air or as exposure rates. The relation between the air absorbed dose rate (Da) and exposure rate is given by:

$$Da = aE \quad (2)$$

where a has the value 0.869 rad/R

O'Brien (1978) has calculated the conversion factors between exposure and absorbed dose for various organs and tissues of the body. The relationship between exposure and whole-body dose (d) measured in rad, is given by:

$$D = 0.6E \quad (3)$$

Different types of radiation cause different effects in biological tissues. For this reason, in comparing the effects of radiation on living systems, a derived unit, the roentgen equivalent man, or rem is used. One rem is the dose from any radiation that produces effects in man equivalent to one rad of X rays. The dose in rems is the product of the dose in rad and a factor which depends on the Relative Biological Effectiveness (RBE) of the radiation considered. This unit of dose is commonly called dose-equivalent (D.E.). Therefore

$$D.E. \text{ (rems)} = RBE \times \text{rad} \quad (4)$$

X rays and gamma rays, which are the principal concern in this report, have an RBE value = 1. In recent years quantities used in radiation protection have more commonly been expressed in System International units; these SI units are the Gray (GY) and the Sievert (Sv). The Gray is the unit of absorbed dose corresponding to the rad and is the energy imparted by ionizing radiation to material corresponding to one joule/kg. The relation between the gray and the rad is:

$$1\text{Gy} = 100 \text{ rad} = 1 \text{ Joule/kg} \quad (5)$$

The Sievert is the SI unit for dose-equivalent corresponding to the rem, the relation is given by

$$1 \text{ Sv} = 100 \text{ rem} \quad (6)$$

## 5. THE RELATIONSHIP BETWEEN RADIOELEMENT CONCENTRATION AND EXPOSURE

It is extremely difficult to evaluate the radiation exposure 1 m above the ground for radioelements of known concentration because the energy distribution of the gamma ray flux of each of the three radioelements must be calculated and there are several hundred gamma ray energies involved by this flux, each with different attenuation coefficients and with multiple scattering occurring both in the ground and air. This difficulty has been overcome with the advent of high speed computers and the energy and angular distribution of both the direct and scattered gamma ray components can now be determined. Beck and de Planque (1968) carried out these calculations at the Environmental Measurements Laboratory in New York for the purpose of evaluating the exposure rate from natural gamma radiation and fallout from nuclear weapons tests. Independently, Kirkegaard (1972) and Lovborg and Kirkegaard (1975) have carried out similar calculations to aid in the interpretation of gamma ray survey for exploration and arrived at similar solutions. Both calculations solve the Boltzman transport equation for two semi-infinite homogeneous media, one being the ground with a uniform distribution of gamma ray emitters, and the other being the air.

Table VI shows the contribution from potassium, uranium and thorium to the exposure rate 1 m above the ground. The agreement between the results of Beck et al. (1972) and Lovborg and Kirkegaard (1974) is a good indication that the energy distribution of the gamma ray flux can be derived reliably.

TABLE VI. CALCULATED CONTRIBUTION OF POTASSIUM, URANIUM AND THORIUM TO THE EXPOSURE RATE 1M ABOVE THE GROUND

	Exposure Rate ( $\mu\text{R/h}$ )		
	Beck et al. 1972	Lovborg, Kirkegaard 1974	Assigned value
K%	1.49	1.52	1.505
1 ppm U <sup>1</sup>	0.62	0.63	0.625
1 pm Th <sup>1</sup>	0.31	0.31	0.31

<sup>1</sup> Assuming radioactive equilibrium

In order to verify the validity of the content of the above Table, Reuter Stokes carried out measurements at four sites along the airborne gamma ray spectrometer calibration range utilizing ionization chamber. Radiation measurements were also taken by a boat on the Ottawa River nearby, to estimate the combined background radiation exposure due to cosmic radiation, airborne radioactivity, and any small component of instrument background. Soil moisture measurements were taken at each site because of the dependence of the gamma ray exposure rate on the moisture content of the soil. Utilizing the assigned radioelement concentration of the Breckenridge of airborne calibration range, the average exposure rate along the test strip due solely to potassium, uranium and thorium was calculated to be  $5.7 \pm 0.12 \mu\text{R/h}$ . This calculated value, however, will vary with the moisture content of the soil. The reduced exposure rate (E) over soil with W per cent soil moisture by dry weight compared to the value E<sub>o</sub> over dry soil, can be considered to be the result of a decrease in radioactive concentration and is given by

$$E = \frac{100 E_o}{100 + 1.11 W} \quad (7)$$

The factor 1.11 arises because water has 1.11 times as many electrons per gram as most rock material and therefore is more effective in attenuating gamma radiation by Compton scattering, which is the predominant attenuation process above about 0.4 Mev.

## 6. A BRIEF ABOUT JORDAN GEOLOGY

Jordan is situated on the northwest flank of the Nubo-Arabian shield, along the eastern flank of the Dead Sea Rift, and on the southern shore of the ancient Tethys Ocean (Fig. 5). The oldest known rocks of Jordan outcrop in its southwestern corner. Since Pre-Cambrian times this granitic shield has remained predominantly a land surface, ringed around by seas which received the erosion product from the land. The shield has pulsed up and down in epeirogenic movement. Minor down beats permitted small ingressions of the sea; the rare major descents resulted in marine transgressions reaching far into the heart of the continent.

The age of these oldest rocks is imprecisely known, they are classified as Proterozoic, they include metamorphosed to unmetamorphosed mafic to felsic igneous rocks and associated sedimentary to metasedimentary assemblages. These are unconformably overlain by Late Precambrian metasedimentary rocks which are intruded by granitic bodies of varying sizes. Unmetamorphosed Cambrian to Silurian sedimentary rocks unconformably overlie the Precambrian. These rocks are predominantly marine but continental sediment occur within the Cambrian, Lower Ordovician and Upper Silurian sequence which dips gently north and northeastward beneath the Mesozoic and Cenozoic sequences. The Paleozoic section consists mostly of clastic, probably derived from the southeast and east. Some relatively thin carbonates occur to the northwest in the Cambrian section

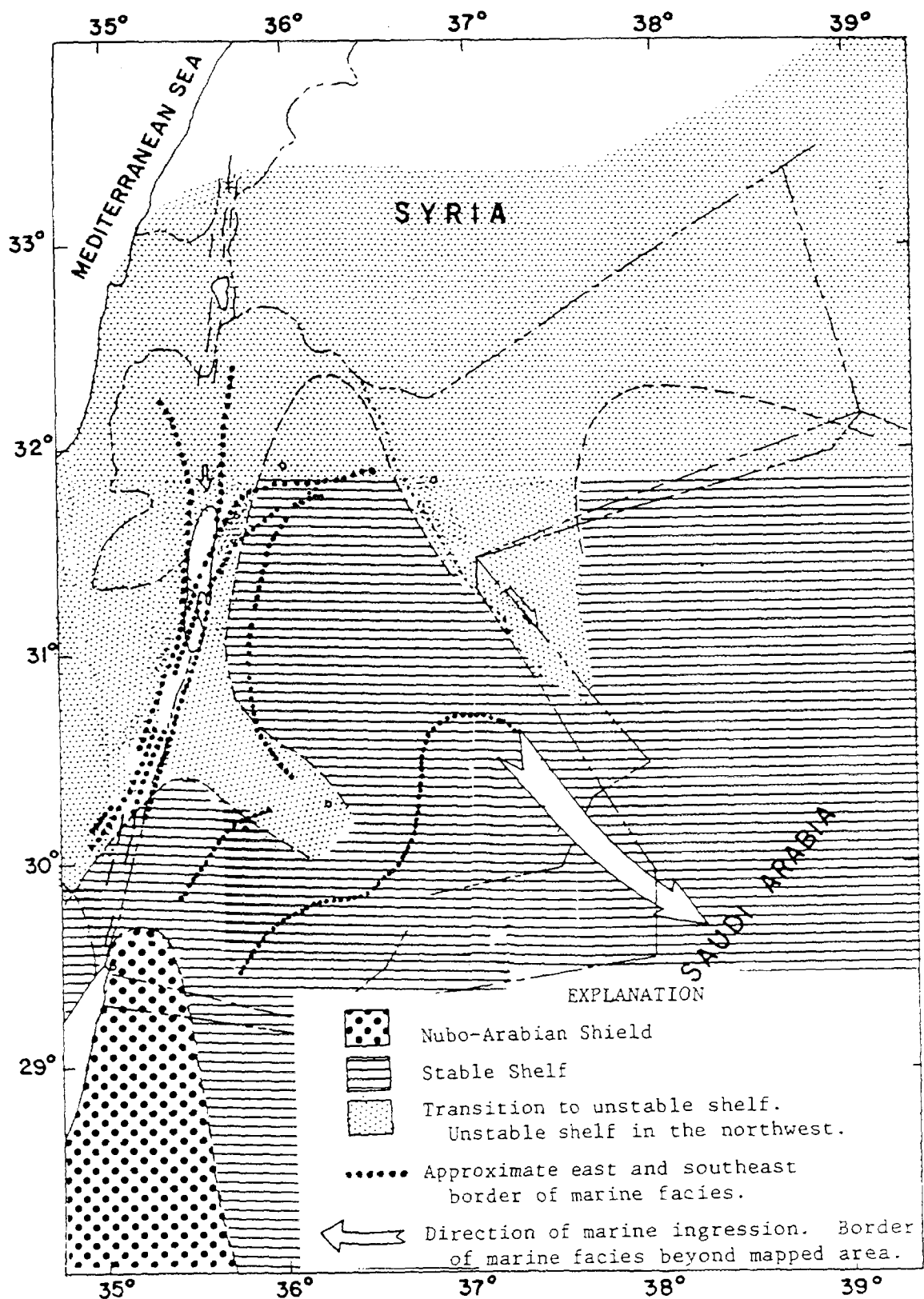


FIG. 5. Regional tectonic setting of survey area (after Bender, 1975).

not far above the base of the sequence, probably representing an abortive attempt to establish a carbonate bank in the early Paleozoic. Younger Paleozoic (Devonian, Carboniferous and Permian) sequences are not known in Jordan.

The post-Paleozoic unconformity bevels the entire section from the exposed Silurian down to the Precambrian. The oldest rocks found above the unconformity are Lower to Middle Triassic rocks representing the first vestige in Jordan of the Mesozoic marine transgression of the Tethys Ocean from the north. Uppermost Triassic rocks are not existing everywhere, and the overlying Jurassic is separated partly from the Triassic by an unconformity, but the sequence are dominated by marine carbonates and clastics. Lower Cretaceous rocks overlie Triassic to the south and the former overlie the Paleozoic and Precambrian further south suggesting extensive uplifting and erosion following the earlier initial marine transgression from the north and northwest during the Triassic and Jurassic. Following the beveling of the pre-Cretaceous rocks, a clean quartz sandstone marked the continental facies of Cretaceous transgression in the southwest, delineating the shoreline over a broad area. Other lithologies occur along the base of the unit farther north and it grades into a coarse brown sandstone to the southeast. Lithologic similarities and the lack of other evidences make it difficult to recognize the unconformity in several places. The widespread deposits of the Upper Cretaceous including a variety of marls, limestones, dolostones and dolomitic limestones are representing the most extensive and dominating northwest to southeast transgression of the Tethys Ocean to date. Carbonate deposition continued until well into the Oligocene. However, widespread deposition of clastics with some calcareous occurred in central, eastern and southern Jordan until the Cenomanian. The widespread phosphate-bearing sediments of economic importance in central and southern Jordan were deposited in a Campanian-Maestrichtian transgression overlap the lower parts of the Upper Cretaceous. Sediments consist of fossiliferous phosphatic limestone and silicified material (both limestone and phosphate), are considerably less silicified than the unit below. Despite its fossiliferous nature there is disagreement about the exact age of this unit. Some place it in the Maestrichtian, while others feel it should be classed as Campanian. Field correlation indicate it is a time-transgressive unit in either case, becoming younger toward the southeast. Some of southeasternmost phosphorite deposits are found in the Paleocene.

Transgressions in the northwest to southeast directions were repeated several times during the Mesozoic as the Tethys Ocean inundated the region and then retreated. The uppermost Cretaceous-lowermost Tertiary thins toward the southeast and becomes a sandier littoral facies. Local thickenings are found in basins having a north to northwest elongation.

Volcanic activity occurred in the western part of Jordan between middle Jurassic and early Cretaceous time. Other mafic to felsic dykes and sills are found in the Wadi Araba region cutting Mesozoic sedimentary rocks, but they could be much younger (Bender, 1974, p.105).

Deposition of limy sediments continued in uninterrupted way from the Cretaceous into the Tertiary. Coarse lenticular-unsorted conglomerates (lower Syntectonic Conglomerates) begin to appear in the section overlying Upper Cretaceous or Tertiary units in the eastern Wadi Araba area. They are in an unconformable relationship in some areas and fossil evidence from several localities indicates their ages may range from Upper Oligocene to Lower Miocene. They are significant that they indicate uplift and probably tectonic activity nearby. A similar conglomerate (Upper Syntectonic Conglomerate) overlies unconformably the lower conglomerate or the older Cretaceous or Tertiary units, always in Wadi Araba region. The age of these upper conglomerates is uncertain and could range from Miocene to Middle Pleistocene (Bender, 1974, p. 92). Their tectonic significance is the same as that of the lower conglomerates. Both sets of deposits probably are related to initial subsidence and block faulting along the Dead Sea Rift. Considerable thickness of marine sediments were deposited throughout the Tertiary in Jordan. However, in some areas uplifting above sea level occurred and brackish water, lacustrine and fluvial deposits were laid down. Also, as part of the Dead Sea Rift opened, over 3.5 km of evaporates were deposited, probably during the late Miocene to early Pleistocene (Bender, 1974, p. 90-91).

Deposits of quaternary age in Jordan reflect continuous uplifting and retreating of the marine environment. More lacustrine and fluviatile occur in this interval than in older sequences. Considerable thicknesses of conglomerates were deposited in and near the Rift during this time. Extensive mafic volcanic and shallow intrusive activity occurred in Jordan and the remainder of the Arabian Peninsula during the Quaternary. While there are four principal modes of occurrence of Quaternary mafic rocks, their locus is Dead Sea Rift. They occur as localized flows and plugs, some tuffs, and as plateau flood of basalts. The latter make up an extensive basalt plateau that crosses northeast Jordan from Syria and continues well into Saudi Arabia.

Basalts which may be directly associated with the Rift are chemically primitive and appear to reflect rapid propagation of fractures into the mantle, then rapid extrusion [Barberi et al., 1979].

## 7. NATURAL RADIOELEMENTS OCCURRENCE IN JORDAN

### 7.1. Uranium

The best occurrence of uranium minerals is that of the phosphorite unit which covers a large part of the Jordan plateau and parts of the highlands as shown on the location map (Fig. 6). The phosphorite section reaches 70 metres in thickness in some locations. It contains disseminated uranium minerals, from which the following have been identified.

Meta-Autunite:  $\text{Ca}(\text{UO}_2)_2(\text{PO}_4)_2 \cdot 8\text{H}_2\text{O}$

Metatuyamunite:  $\text{Ca}(\text{UO}_2)_2(\text{VO}_4)_2 \cdot 3\text{H}_2\text{O}$

Uranophane:  $\text{Ca}(\text{UO}_2)_2(\text{SiO}_3)_2 \cdot 2(\text{OH}) \cdot 2.5\text{H}_2\text{O}$

Uranium minerals are distributed vertically through the whole phosphorite section. But their concentration varies with depth and lithology, although generally the highest concentrations are in the uppermost phosphate beds.

Hundreds of samples have been analysed on the basis of gamma ray of logging and scintillometric measurements and a relationship between gamma radiation and uranium oxide has been established accordingly, as indicated in (Fig. 7). The zoning in the uranium content is also correlated with lithology.

The phosphorite section of Fig. 8 represents most of the upper-Cretaceous (Campanian-Maestrichtian) in east Jordan. This cross-section is divided to the following zones according to their radioactivities.

1. The moderate radioactive zone 1 (M.R.Z.I): It consists of marl that overlies the phosphate, sometimes it is completely eroded, its age is estimated as Danian-Paleocene. Its  $\text{U}_3\text{O}_8$  in average is 95 ppm.
2. The strong radioactive zone (S.R.Z.): It is the upper minable phosphate series and contains a thin marl band on its top. Its  $\text{U}_3\text{O}_8$  in average is about 204 ppm.
3. The moderate radioactive zone II (M.R.Z.II): It consists of the lower part of the upper  $\text{U}_3\text{O}_8$  ab-The very low radioactive zone (V.L.R.Z.): It consists of oyster beds that phosphate series and the intercalated marl. Its  $\text{U}_3\text{O}_8$  is about 90 ppm.
4. The very low radioactive zone (V.L.R.Z.): It consist of oyster that have been reworked and is known as the coquina beds of variable thickness about 24 metres. Its have out 90 ppm.
5. The lower phosphate series (M.R.Z.III) which underlies the coquina beds. Its  $\text{U}_3\text{O}_8$  is about 100 ppm.

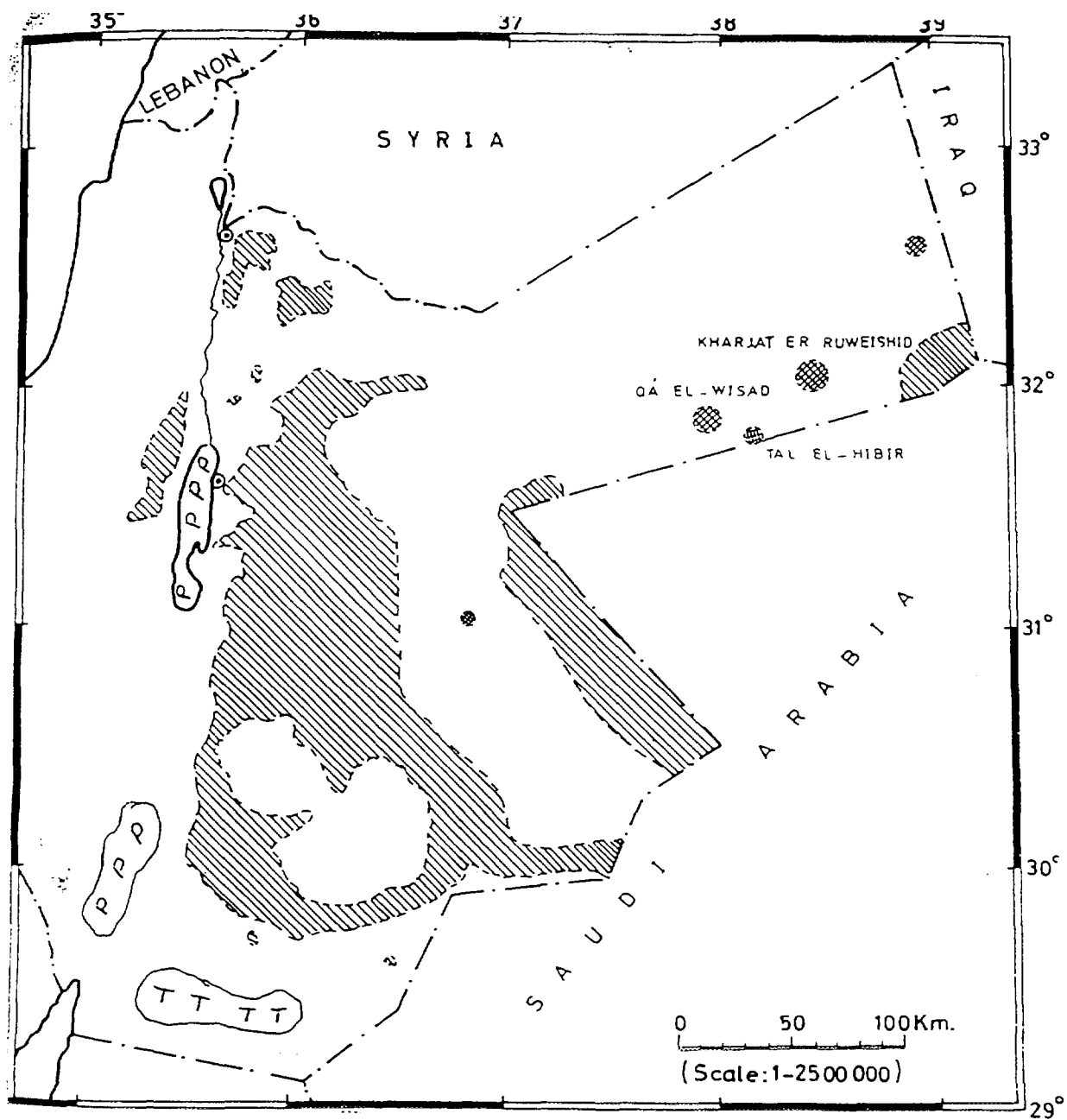
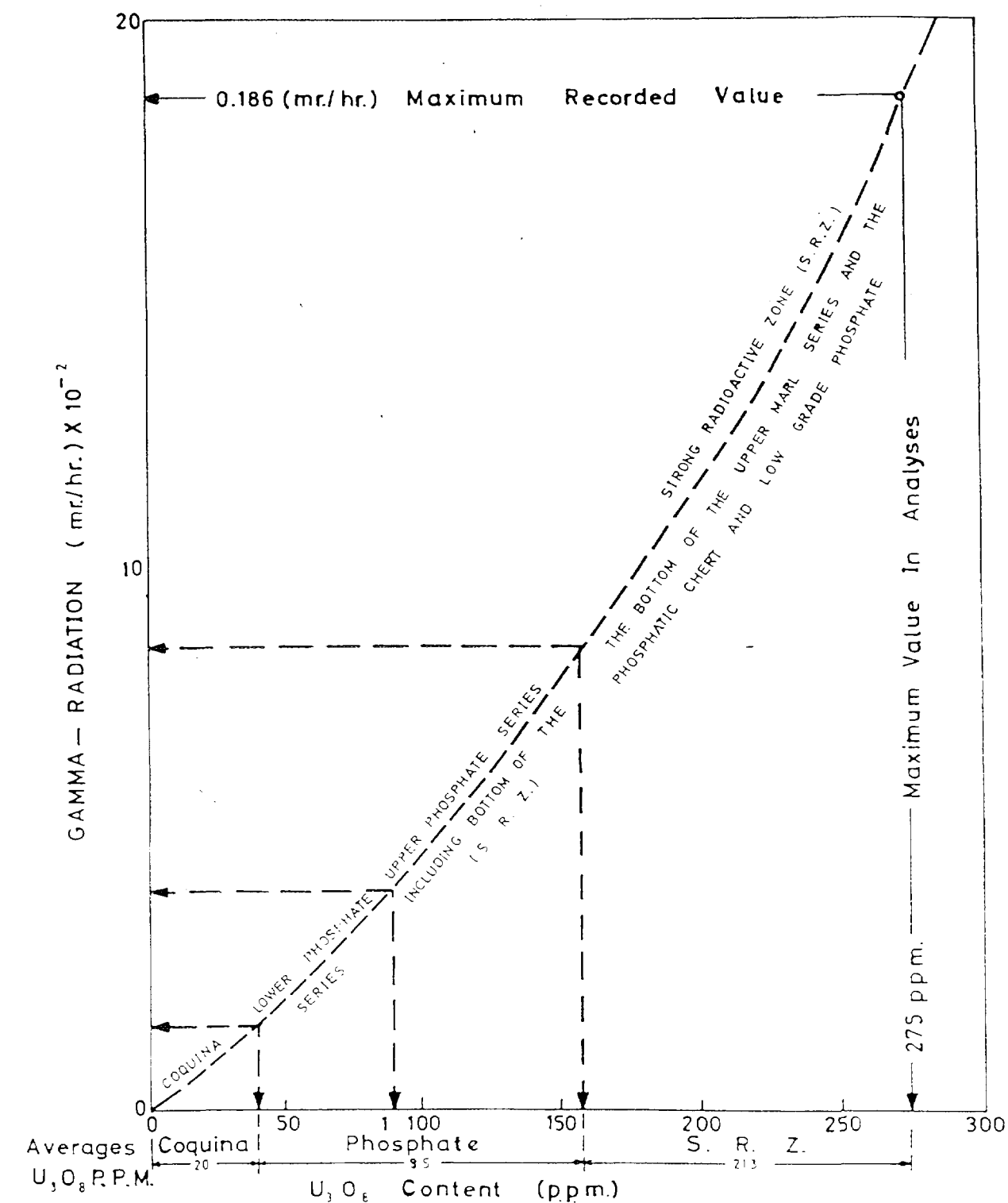


FIG. 6. Natural Radioelements Occurrence in Jordan

# URANIUM EQUIVALENTS IN EL-HASA PHOSPHORITE UNIT

( AN INTERPRETATION OF GAMMA - RAY LOGS AND THE X - RAY FLUORESCENCE ANALYSES OF BORE SAMPLES



Note: THIS DIAGRAM IS AN APPROXIMATE MATCHING OF AVAILABLE DATA CALCULATED ERROR IN RADIATION: 2  
CALCULATED ERROR IN EQUIVALENT  $U_3O_8$  PPM. = 1.4%.

FIG. 7. Uranium equivalents in El-Hasa phosphorite unit (from Abu Ajamieh 1974).

# CHARACTERISTIC SUBSURFACE SECTION

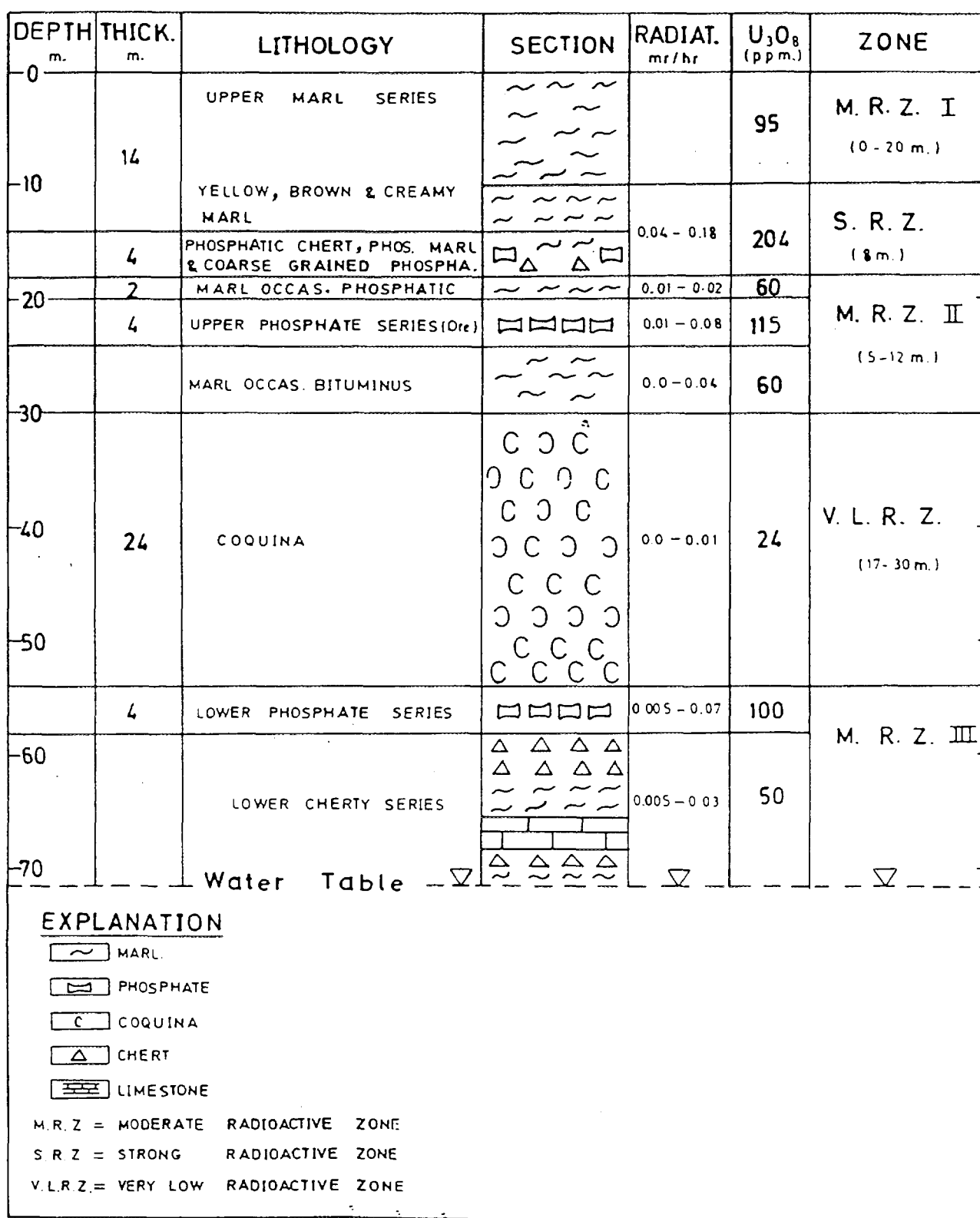


FIG. 8. Average cross section of subsurface geological and radiometric analyses data in the area between Suwaqa and Jurf Addarawish (from Abu Ajamieh 1974).

6. The lower cherty series: which consists of an alternation of chert, limestone and marl or thin low grade phosphate. Its  $U_3O_8$  is about 50 ppm. This zone is the top of the regional aquifer.

## 7.2. Thorium

Thorium is typically present in crustal materials in concentrations of between 3 to 4 ppm. However, Phosphate mineral is poor in thorium concentrations as the case of Jordan Phosphate. Thorium is present in Jordan within the Paleozoic section in southeastern Jordan. It occurs within the fine-grained marine sandstone and shale unit of Llanvirn age in the Ordovician. It is found associated with uranium and zircon mineral in a metamict state. Its concentration reaches sometimes 2000 ppm.

## 7.3. Potassium

Potassium has a simple form of radioactive decay, only  $^{40}K$  of several natural isotopes of potassium is radioactive. It has a relative isotopic abundance of only 0.018%.

The average concentration of potassium in crustal rocks ranges from 0.1 to 5% Jordan is rich in this element. The concentration of this element reaches about 7.5% in the Dead Sea salty water. It is present as KCl mineral. Potassium also exist in southern Jordan, it is found with associated with orthoclase feldspar (K feldspar).

TABLE VII. DIGITAL ARCHIVE TAPE

Digital Archive Tape	
Tape density	9 Track, 1600 BPI
Code	EBCDIC
Physical Blocksize	17600 bytes (fixed)
Logical record length	176 bytes

Content of a single logical record — Format (2218)

1. Identifier = flight $\times 10 \exp 6$ + line $\times 10 \exp 2$ + part	11. IGRF value (gamma $\times 100$ )
2. Fiducial	12. Raw total count (cps)
3. Time (seconds $\times 10$ past midnight)	13. Raw potassium (cps)
4. Residual magnetics (gamma $\times 100$ )	14. Raw uranium (cps)
5. X (UTM)	15. Raw thorium (cps)
6. Y (UTM)	16. Final total count (cps)
7. Radar altimeter (metres)	17. Final potassium (cps)
8. Barometric altimeter (gamma $\times 100$ )	18. Final uranium (cps)
9. Raw magnetics (gamma $\times 100$ )	19. Final thorium (cps)
10. Compensation value (gamma $\times 100$ )	20. uranium/thorium
	21. uranium/potassium
	22. thorium/potassium

## 8. DATA VALIDATION AND EXPOSURE AND DOSE RATES CALCULATION

The whole field data (raw and processed) are available at Natural Resources Authority archives. The processed data are as described in Table VII, they are recorded on residual archive

tapes which contain the counts/second and the ratios for K, U, and Th. The tapes were down loaded to the Unix system and then the wanted columns (coordinates and corrected counts/second for K, U, and Th) are extracted from other data by using an appropriate program.

The data were checked to find any possible error in coordinates or values using the Geosoft software, some points were rejected because of wrong coordinates and many of data were rejected because of negative counts/second values.

Assumed that the data is now free of errors the counts per second were divided by 7.7, 4.8 and 66.5 which represent the sensitivity of the Harshaw crystal for U, Th and K respectively (see Table V). The results obtained by these divisions are the concentrations at the ground level expressed in ppm for uranium and thorium and in percentage for potassium.

In order to find the exposure rate expressed in  $\mu\text{R/h}$ ; the ground concentrations for K, U and Th are multiplied by the factors 1.505, 0.625 and 0.31 respectively as indicated in Table VI. The values obtained were added together and the total exposure rate due to the natural radioelements is thus obtained.

In order to find the dose rate expressed in  $\mu\text{Sv/h}$ , the exposure rate is divided by 100 and multiplied by 0.6 as indicated by equation (3).

## 9. MAP CONTOURING

The values of exposure rate and dose rate were gridded with grid cell size equal 500 m using the Geosoft software. Values were smoothed using two passes of Hanning filter in order to get rid of noisy values which due to bad topography or difficulty in maintaining the same aircraft altitude or due to equipment noise or other sources of errors. The exposure rate reached a value as high as  $46 \mu\text{R/h}$  in El-Hasa area where there are Phosphate mines and dose rate equivalent to  $0.276 \mu\text{Sv/h}$ , these values are corresponding to  $380 \text{ mR/y}$  and  $2.3 \text{ mSv/y}$ , see exposure rate and dose rate map for Jordan.

## 10. MAP ANALYSIS

In spite of that the map represent the contribution of the three natural radioelements all together but it reflects the surface geology of Jordan where the phosphate deposition is very well delineated by the high radiation contours in the central part of Jordan. Jordan phosphate contain about 200 ppm of uranium with practically no thorium and very low content of potassium and covers almost the whole the eastern high plateau of Jordan. In eastern Jordan parallel to Saudi Arabia borders, the exposure radiation map does not show good indication of the phosphorite occurrence in this region because the phosphate has low uranium content in this region. In northern Jordan, the phosphate deposition is very well indicated by the radiation exposure map, while in the far north east of Jordan the exposure map is less indicative of phosphate occurrence in this region, this because the recent sedimentation covers the phosphorite units and prevent gamma radiation from escaping into the space and therefore less detection by airborne radiometric survey, also the exposure rate map Fig. 9 shows medium two high radiation areas, one at the eastern coast of the Dead Sea, this because of Main and Zara hot springs which is caused by radon emanation carried by underground circulating waters through different rock types.

The other one in southern Jordan between Quweira and Mudawwara villages at Dubeidib area. This area proved the existence of high concentration of thorium in the Ordovician sandstones which reach about 2000 ppm in some locations associated with a medium to high concentrations of uranium (100 to 500) ppm in a metamict state.

Comparing Fig. 9 with Fig. 6, good match is noticed between the two maps, which means high concentration in one of the three radioelements leads to the contribution of high radiation exposure to the environment of results.

## 11. DISCUSSION OF RESULTS

Jordan shows high radiation exposure in its central part of Jordan where the phosphate deposition occur. Most of Jordan phosphates are covered by recent sedimentations, such as oil shale and chalky marl depositions of Upper Cretaceous age their thicknesses reach about 15 to 20 metres in some locations. The detected radiation by airborne survey are only those which outcropping in some places or uncovered by phosphate mining. The level of radiations already high despite the fact that the survey lines were separated of 2 km from each other which might lead not passing over the Phosphate Mines or missing many of open casts of Phosphate Mines in the phosphate mining area and also without taking into considerations the effect of radiation caused by cosmic rays or caused by internal radiation as discussed early in this report. Off the total of 343 894 measurements were taken by airborne survey, there are about 500 readings exceeding  $20 \mu\text{R/h}$  and about 13 300 measurements exceeding the value 10 and there are several readings as much high as  $45 \mu\text{R/h}$ , all these readings are found in the vicinity or around the Phosphate Mines.

Comparing these results to those obtained in some other countries such as the United States, Germany, Poland, Italy, etc. (see Fig. 10, the exposure rate in Jordan is higher than those of other countries

## 12. CONCLUSION AND RECOMMENDATIONS

Airborne radiometric survey proved to be a very good tool in estimating the ground level exposure rate easily and with an accepted accuracy especially after the creation of very voluminous sodium iodide crystals and the establishment of the calibration concrete pads and with the continuous improvements of signal to noise electronic devices. The airborne radiometric survey is very representative to the area under studying because of the enormous amount of data that cover a wide area. As it is shown previously Jordan has high background radiation. This high background radiation is related to the effect that a vast areas of Jordan high plateau are covered by phosphate deposition which has about 150 ppm in average of uranium. The maximum value of uranium concentration registered in phosphates unit according to Abu Ajamieh (1974) was 275 ppm. Recently in the areas surrounding the Phosphate belt, new investigations proved the existence of high uranium concentration of about 1000 ppm in the recent sedimentations of chalky marl type that overlie the phosphorous and oil shale layers; according to the exposure rate map shows an average exposure rate value of about  $20 \mu\text{R/h}$  in Phosphate belt and the surrounding areas, this corresponds to a dose equivalent of about  $0.12 \mu\text{Sv/h}$  or about  $1 \text{ mSv/y}$ . This value does not consider the area of open mines after uncovering the overlying sedimentations where the thickness of these overlying layers have a thickness of about 30 metres in some locations. Now if we imagine that the whole phosphate belt is outcropping as the case of open cast mines, simple calculations lead us to the conclusion that an extending superficial of Phosphate area with a concentration in uranium of 150 PPM of uranium will contribute an exposure rate to the environment, and according to the table no. (6), of about  $97 \mu\text{R/h}$  neglecting the contributions coming from other radioelements which will be very low because Jordan Phosphate has low concentrations in thorium and potassium. The  $97 \mu\text{R/h}$  corresponds to a dose rate of about  $5 \text{ mSv/y}$ . This figure without doubt is detrimental to human being. If we return back to the figure  $20 \mu\text{R/h}$ , this figure is neglecting any other contributions coming from cosmic rays which is expected to be high because of dry weather in Jordan which permits to the cosmic rays to penetrate the atmospheric cover with less attenuation, or because of the inhalation of the radon gas during breathing (especially the dry climate help radon gas to be emanated and collided to the dust particulates which are abundant in dry countries) or taking any kind of radioactive elements contained with food or water. Comparing the value of  $20 \mu\text{R/h}$  to those obtained from other countries such that the United



*FIG. 9. Radiation exposure rate map of Jordan. Scale 1:2 500 000. MINISTRY OF ENERGY AND MINERAL RESOURCES, Nuclear Energy Directorate, Natural Radiation Exposure Rate Map, Jordan, Radiation Unit:  $\mu\text{R/h}$ , Contour Interval 1  $\mu\text{R/h}$ .*

States, Germany, Italy, Canada, etc. (see Fig. 10). Jordan shows higher radiations than all other countries.

This study illustrated the following to be recommended:

- More detailed studies should be presumed in Jordan so as to determine the radiation exposure rates originating from the external and internal resources.

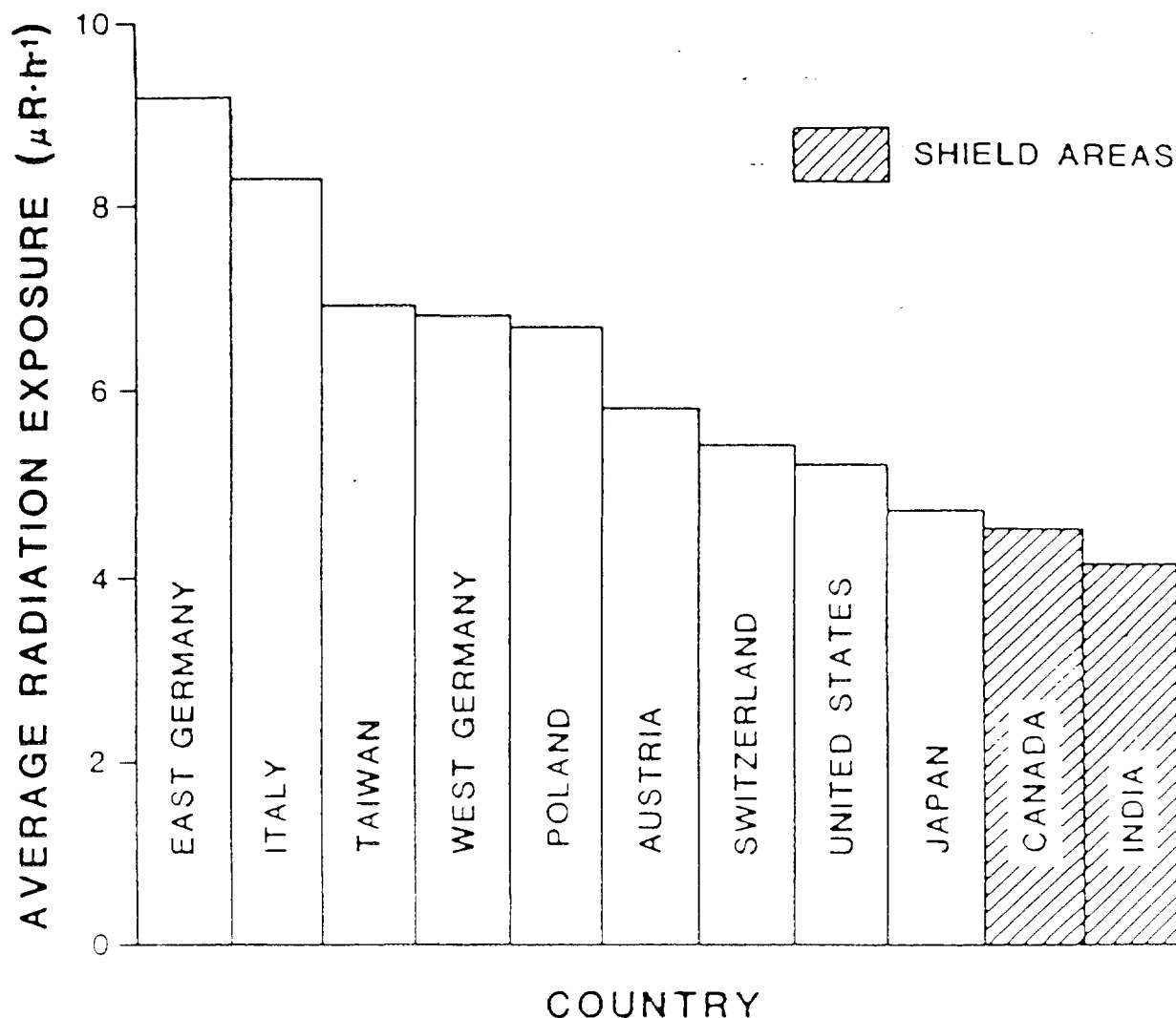


FIG. 10. Outdoor exposure rates for some countries.

- The radiations from every individual natural radioelement should be calculated separately in order to make better estimation to the radiations originated from the uranium which is the primary responsible of high background radiation in Jordan and more care should be paid to the ratios between the three different radioelements because these ratios are good control of the reliability of the data.
- Radiological risks studies should be made on those people who are residing in the Phosphate belt which extends over a vast area in Jordan. and detailed studies should be done on those people who are working in Phosphate Mines.

#### ACKNOWLEDGEMENTS

I am particularly grateful to thank the Director of the Nuclear Energy Director of the Ministry of Energy and Mineral Resources of Jordan for his fruitful suggestions and help. I am also grateful to thank the following for their great help: Geophysicist Abdulrahman Abu El-Adas, Geophysicist Hani Akrabawi, Geophysics Eng. Wajdi El-Tamimi.

## **BIBLIOGRAPHY**

**ABDULKADER M. ABED**, Geology of Jordan (1982).

**BENDER, F. et al.**, "Geology of Jordan" Berlin, Gebrüder Borntraeger (translated by M. K. Khdeir, D.H. Parker, and U. Wilkening), (1969).

**BURDON, D.J.**, Handbook Of the Geology Of Jordan (1959).

**GRASTY, R.L., CARSON, C.M., CHARBONNEAU, B.W., HOLMAN, P.B.**, Natural Background Radiation in Canada, Bulletin 360 (1980).

**INTERNATIONAL ATOMIC ENERGY AGENCY**, Construction and Use of Calibration Facilities for Radiometric Field Equipment, Technical Report Series No. 309, Vienna (1989).

**INTERNATIONAL ATOMIC ENERGY AGENCY**, Gamma Ray Surveys in Uranium Exploration, Technical Reports Series No. 186, Vienna (1979).

**MOHAMMAD ABU AJAMIEH**, Uranium Reserves in Jordan (1974).

**PHOENIX CORPORATION**, A comprehensive Airborne Magnetic/Radiation Survey of the Hashemite Kingdom of Jordan (1980).

## APPENDIX 1.

### Algorithm of Calculations

#### A) Normalize all recorded radiometric channel data to 1 second sampling interval.

$$\begin{aligned}TC_n &= TC_r \times 1/L_T \\K_n &= K_r \times 1/L_T \\U_n &= U_r \times 1/L_T \\Th_n &= Th_r \times 1/L_T\end{aligned}$$

$L_T$  - recorded live time in milliseconds  
Subscript "r" refers to raw recorded data  
Subscript "n" refers to normalized data

#### B) Reduce terrain clearance to the effective value at zero Celsius degree

$$\Delta H2 = H \times 273/(T+273) - H_p$$

$$\Delta H1 = H \times 293/(T+273) - H_p$$

where  $\Delta H1$  = departure from planned survey height,  $H_p$  corrected to 20 Celsius degrees for correcting of U/Th stripping ratio,

$\Delta H2$  = departure from planned survey height,  $H_p$  corrected to 20 celsius degrees for attenuation corrections.

$H$  = terrain clearance in feet or meters

$T$  = ambient temperature in celsius degrees

$H_p$  = planned survey height.

#### C) Correction for Background

$$\begin{aligned}TC_b &= TC_n - B_{TC} \\K_b &= K_n - B_k \\U_b &= U_n - B_u \\Th_b &= Th_n - B_{th}\end{aligned}$$

$B_{TC}$ ,  $B_k$ ,  $B_u$ ,  $B_{th}$  -background values for TC,K,U,Th

Subscript "b" refers to backgroun corrected data

Subscript "n" refers to normalized data

The background value at any time is linearly interpolated between known background corrected segments.

#### D) Altitude correction of stripping coefficients

Geoterrex practice has been to correct one stripping coefficient, ALPHA( $\alpha$ ), for latitude following the technique outlined by Grasty.

$$ALPHA_H = ALPHA + 0.0373 + 0.000076 \times \Delta H1$$

ALPHA - Th into U stripping ratio at ground level

ALPHA<sub>H</sub> - Height corrected ALPHA

0.0373 and 0.000076 -constants theoretically determined by the Geological Survey of Canada.

### E) Spectral Stripping

$$U_s = (U_b - \text{ALPHA} \times Th_b) / (1 - a \times \text{ALPHA})$$

$$Th_s = (Th_b - a \times U_b) / (1 - a \times \text{ALPHA})$$

$$K_s = K_b - \gamma \times U_s - \beta \times Th_s$$

$$TC_s = TC_b$$

Subscript "b" refers to background corrected data

Subscript "s" refers to stripped data

a = U into Th backstripping ratio

$\beta$  = Th into K stripping ratio

$\gamma$  = U into K stripping ratio

### F) Altitude Correction of the Data

$$TC_a = TC_s \times e^{(\mu_{TC} \times \Delta H_2)}$$

$$K_a = K_s \times e^{(\mu_K \times \Delta H_2)}$$

$$U_a = U_s \times e^{(\mu_U \times \Delta H_2)}$$

$$Th_a = Th_s \times e^{(\mu_{Th} \times \Delta H_2)}$$

where  $\mu_{TC}$ ,  $\mu_K$ ,  $\mu_U$ ,  $\mu_{Th}$  are total count, Potassium, Uranium and Thorium attenuation coefficients

Subscript "s" refers to stripped data.

Subscript "a" refers to attenuated data.

The data submitted by Phoenix Corporation To Natural Resources Authority were not reduced to indicate %K, ppm U and ppm Th, but were compiled in counts per second(cps) response. The ratios of U/Th, U/K and Th/K were computed.

**NEXT PAGE(S)  
left BLANK**